

## Electronic Supplementary Information

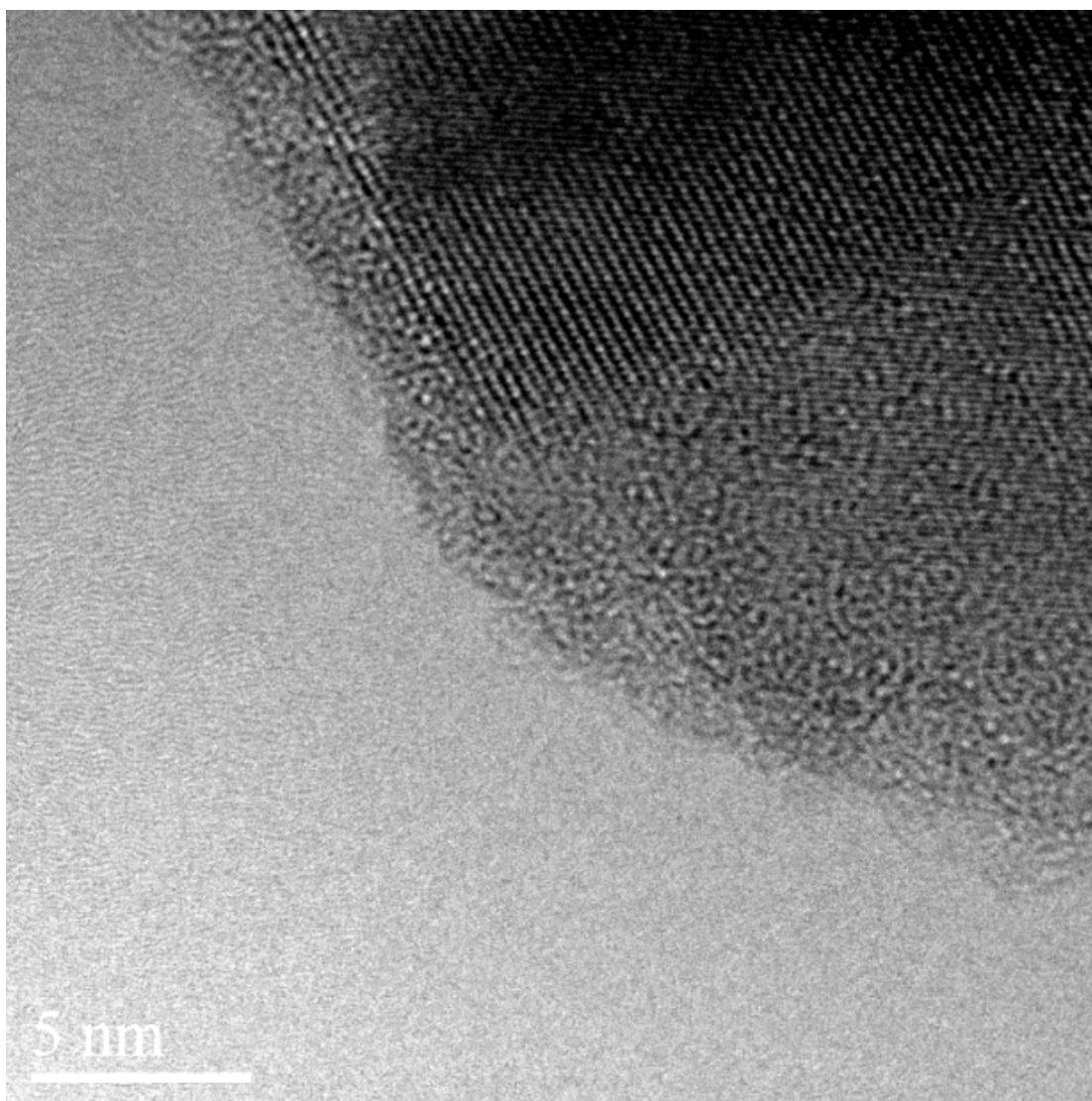


Fig. S1 The HRTEM image of Si@u-SiO<sub>x</sub>-NH<sub>2</sub> obtained by one-step method for 24h.

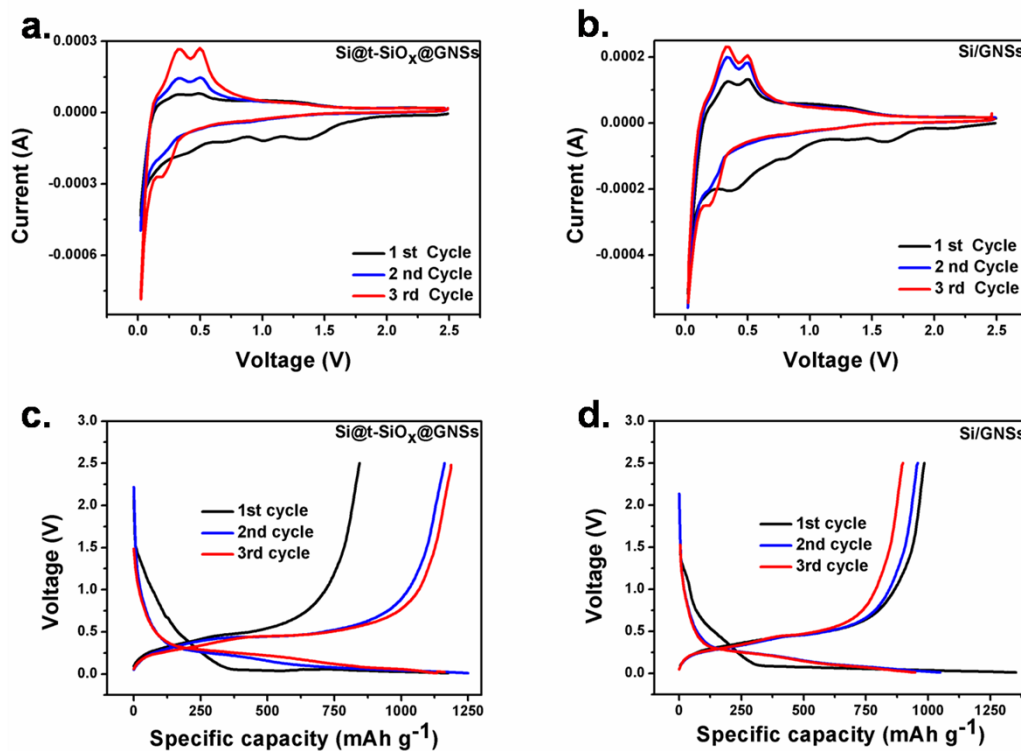


Fig. S2

CV curves of (a) Si@t-SiO<sub>x</sub>@GNSs and (b) Si/GNSs as anode material for LIBs; charge-discharge plots of (c) Si@t-SiO<sub>x</sub>@GNSs and (d) Si/GNSs.

Fig. S2a and S2b show the first three cyclic voltammetry (CV) curves of Si@t-SiO<sub>x</sub>@GNSs and Si/GNSs. The reduction current in the first cycle above ~0.3V is larger than that of the following two cycles. The additional current could be assigned to the electrolyte being irreversibly reduced to form SEI. The additional current can also be seen from the CV curves of Si@u-SiO<sub>x</sub>@GNSs. However, other peaks are so strong that obscure this broad reduction peak. The phenomenon that the peak around 0.21V does not exist in the first cycle but gradually evolves in the subsequent cycles also occurs in the CV curves of Si@t-SiO<sub>x</sub>@GNSs and Si/GNSs, and this reduction peak of Si@u-SiO<sub>x</sub>@GNSs in the second cycle is stronger than those of Si@t-SiO<sub>x</sub>@GNSs and Si/GNSs. This also indicates that the Li extraction kinetics of former is better than those of latter two. Other reduction and oxidation peaks from CV curves of Si@t-SiO<sub>x</sub>@GNSs and Si/GNSs are consistent with those of Si@u-SiO<sub>x</sub>@GNSs. The cathodic part of the second cycle shows two peaks: at 0.05V and 0.21V, corresponding to the formation of Li-Si alloy phases. The anodic part displays two peaks, at 0.31V and 0.5V, corresponding to the de-alloying of the Li-Si alloys, consistent with previous reports<sup>1,2</sup>. The detailed charge-discharge plots of Si@t-SiO<sub>x</sub>@GNSs is given in Fig. S2c. The lithiation is not complete at the first cycle so that the second charge capacity increases by 313.8mAh g<sup>-1</sup>. This indicates that the thick silica shell in Si@t-SiO<sub>x</sub>@GNSs limits the lithiation. From the detailed charge-discharge process of Si/GNSs (Fig. S2d), we can see that the cycle performance of Si/GNSs is poor which can be attributed to that unmodified Si nanoparticles cannot be well encapsulated by GNSs.

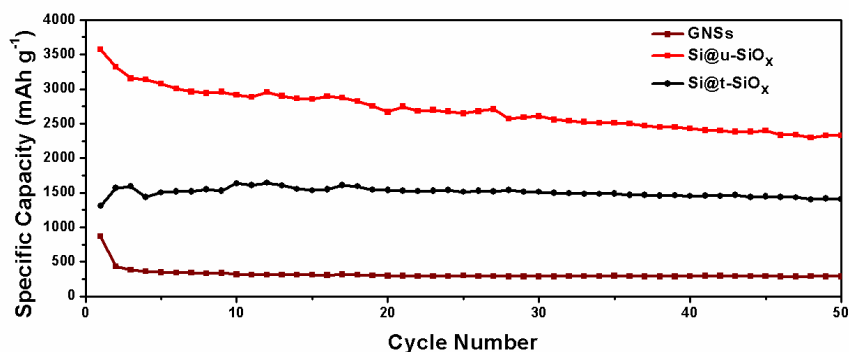


Fig. S3 Cycling performance of GNSs and calculated capacity retention of the Si@u-SiO<sub>x</sub> and Si@t-SiO<sub>x</sub> alone.

GNSs were obtained by direct thermal reduction of graphene oxide at 750 °C for 2 h. Then, GNSs were used as anode material for LIBs.

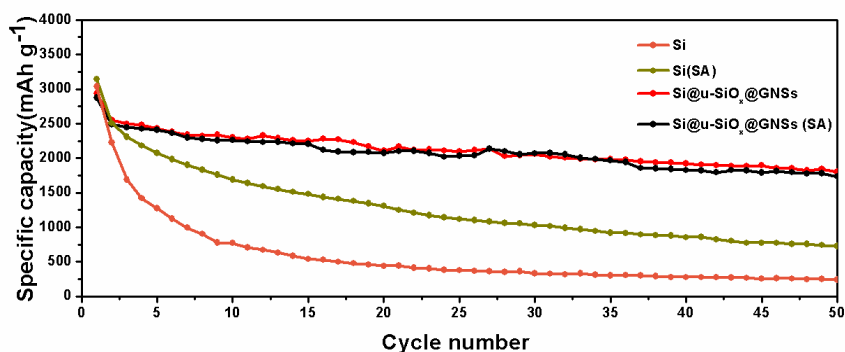


Fig. S4 Cycling performance comparison of Si nanoparticles and Si@u-SiO<sub>x</sub>@GNSs with PVDF and SA binders.

Fig. S3 shows the cycling performance comparison of Si nanoparticles and Si@GNSs with PVDF and sodium alginate (SA) binders. SA has been reported to markedly improve the electrochemical performance of silicon anodes<sup>3-5</sup> and the improvement can be seen clearly from Fig. S3. However, the cycle performance shown by Si@u-SiO<sub>x</sub>@GNSs with SA binder is similar to that with PVDF binder. The good cycling capability with both SA and PVDF binders indicates the structure of Si@u-SiO<sub>x</sub>@GNSs we prepared is superior.

Table S1. Summary of the fabrications and electrochemical performance of Si/GNSs anode materials for LIBs through electrostatic self-assembly method in recent years.

Precursors for self-assembly and posttreatment	1st discharge/ charge capacity and Initial CE <sup>a</sup>	Cycling performance	Rate capability	Binder	Reference
Si@ultrathin SiO <sub>x</sub> -NH <sub>2</sub> (+) and GO (-) Thermal reduction	2933/2391 mAh g <sup>-1</sup> 81.5%	1844 mAh·g <sup>-1</sup> after 50 cycles at 200 mA·g <sup>-1</sup>	1673, 1297, 929 mAh·g <sup>-1</sup> at 500,1000, 2000 mA·g <sup>-1</sup> 700 mA·g <sup>-1</sup> after 350 cycles	PVDF	This work
Si@SiO <sub>x</sub> -PDDA <sup>b</sup> (+) and GO (-) Thermal reduction and HF etching	2920/1720 mAh g <sup>-1</sup> 58.9%	1205 mAh·g <sup>-1</sup> after 150 cycles at 100 mA·g <sup>-1</sup>	1452, 1320, 990 mAh·g <sup>-1</sup> at 400,800, 1600 mA·g <sup>-1</sup>	PVDF	1
Si@SiO <sub>x</sub> (-) and GO/DODA (+) chemical reduction by N <sub>2</sub> H <sub>4</sub>	3559/1686 mAh g <sup>-1</sup> 47.4%	1118 mAh·g <sup>-1</sup> after 50 cycles at 50 mA·g <sup>-1</sup>	1139, 925, 664, 491 mAh g <sup>-1</sup> at 100, 200, 500, 1000 mA g <sup>-1</sup>	NO	2
Si <sup>c</sup> @SiO <sub>x</sub> -APTES (+) and GO (-) Thermal reduction and HF etching	2142/1649 mAh g <sup>-1</sup> 80%	1335 mAh·g <sup>-1</sup> after 80 cycles at 200 mA·g <sup>-1</sup>	1090, 701, 441 mAh·g <sup>-1</sup> at 500,1000, 5000 mA·g <sup>-1</sup>	PVDF	6
Si@SiO <sub>x</sub> (-) and N-doped graphene (+)	~5500/2500 mAh g <sup>-1</sup> 47%	~1000 mAh·g <sup>-1</sup> after 100 cycles at 210 mA·g <sup>-1</sup>	~800 and 300 mAh·g <sup>-1</sup> at 1.2 and 12.1A·g <sup>-1</sup>	PAA <sup>d</sup>	7
Si-COOH (-) and G-PIL <sup>e</sup> (+) Thermal reduction	~1250/900 mAh g <sup>-1</sup> ~72%	987 mAh·g <sup>-1</sup> after 50 cycles, 803 mAh·g <sup>-1</sup> after 100 cycles at 200 mA·g <sup>-1</sup>	1100, 870, 735 at 400, 800, 1600 mA·g <sup>-1</sup>	CMC <sup>f</sup>	8
PANI-Si <sup>g</sup> (+) and GO(-) Thermal reduction	~2200/1600 mAh g <sup>-1</sup> 73.2%	1400 mAh·g <sup>-1</sup> after 50 cycles at 100 mA·g <sup>-1</sup>	900 mAh·g <sup>-1</sup> at 2A g <sup>-1</sup> after 300 cycles	PVDF	9

<sup>a</sup>CE: Coulombic efficiency. <sup>b</sup>PDDA: poly(diallyldimethylammonium chloride). <sup>c</sup>Si: Si nanowires.  
<sup>d</sup>PAA: poly (acrylic acid) binder which can considerable improve the electrochemical performance of Si nanoparticles.  
<sup>e</sup>G-PIL: graphene-modified protic ionic liquid.  
<sup>f</sup>CMC: carboxymethylcellulose binder which can also improve the electrochemical performance of Si nanoparticles.  
<sup>g</sup>PANI-Si: polyaniline grafted Si nanoparticles.

References:

- 1 X. Zhou, Y. X. Yin, L. J. Wan and Y. G. Guo, *Advanced Energy Materials*, 2012, **2**, 1086.
- 2 H. Tang, J.-P. Tu, X.-Y. Liu, Y.-J. Zhang, S. Huang, W.-Z. Li, X.-L. Wang and C.-D. Gu, *J. Mater. Chem. A*, 2014, **2**, 5834.
- 3 Y. Wen, Y. Zhu, A. Langrock, A. Manivannan, S. H. Ehrman and C. Wang, *Small*, 2013, **9**, 2810.
- 4 C. Sun, Y. Deng, L. Wan, X. Qin and G. Chen, *ACS Appl. Mater. Interfaces*, 2014, **6**, 11277.
- 5 I. Kovalenko, B. Zdyrko, A. Magasinski, B. Hertzberg, Z. Milicev, R. Burtovyy, I. Luzinov and G. Yushin, *Science*, 2011, **334**, 75.
- 6 Y. Zhu, W. Liu, X. Zhang, J. He, J. Chen, Y. Wang and T. Cao, *Langmuir*, 2013, **29**, 744.
- 7 W Lee, T Hwang, J Hwang, H Kim, J Lim, H Jeong, J Shim, T Han, J Kim, J Choi and S Kim. *Energy Environ. Sci.*, 2014, **7**, 621.
- 8 Y.-S. Ye, X.-L. Xie, J. Rick, F.-C. Chang and B.-J. Hwang, *J. Power Sources*, 2014, **247**, 991.
- 9 Z.-F. Li, H. Zhang, Q. Liu, Y. Liu, L. Stanciu and J. Xie, *ACS Appl. Mater. Interfaces*, 2014, **6**, 5996.